

Soft-x-ray induced fluorescence of gas mixtures

E. V. Grabovskii, Yu. K. Zemtsov, S. A. Komarov, A. I. Loboiko, G. B. Lopantseva, A. P. Morovov, A. I. Pavlovskii, V. P. Smirnov, A. N. Starostin, A. N. Subbotin, M. D. Taran, and M. V. Tulupov

State Committee on the Use of Atomic Energy

(Submitted 6 September 1991)

Zh. Eksp. Teor. Fiz. **101**, 878–894 (March 1992)

A physical-mathematical model is proposed for the interaction of a soft-x-ray pulse with the mixture of gases $N_2:H_2$. The following processes are taken into account: dissociation of molecules by electron impact, ionization of molecules and atoms by electron impact, photoionization with branching into fragments, dissociative recombination, charge exchange of molecular and atomic ions on hydrogen molecules and atoms, conversion of ions into more complicated ions, and excitation of radiating states of this mixture. The heating of the gas mixture by elastic collisions of electrons with molecules and atoms is taken into account. The model agrees satisfactorily with experiment.

INTRODUCTION

One method for measuring x-ray fluxes is to record the optical fluorescence of gases.¹⁻³ Investigations performed with the Angara-5 setup showed that when wire and gas liners are compressed by ponderomotive forces a pulse of soft x-rays (SXR) with total energy ≈ 100 kJ and width ≈ 30 ns is produced.⁴⁻⁶ Energy fluxes in soft-x-ray pulses can be measured with the help of the optical fluorescence of the gases ionized by the incident radiation. To describe the mechanisms of fluorescence of gases under such conditions, we propose in this paper a physical-mathematical model of the kinetics of ionization and excitation of the radiative states of $N_2:H_2$ mixtures by an external source of x-rays. The computed intensities of optical fluorescence of the gas mixture agree satisfactorily with the experimental results. Our method is sensitive to the composition of the gas mixture and can be employed to record the energy and spectral composition of x-rays.

1. MODEL OF IONIZATION KINETICS

In solving the ion kinetic equations the following processes were taken into account: photoionization with branching into fragments, ionization and dissociation of molecules by electron impact, dissociative recombination, charge exchange of atomic and molecular ions on hydrogen molecules and atoms, and conversion of hydrogen and nitrogen ions into more complicated ion types of (NH^+, N_2H^+) . We shall examine all these processes in greater detail.

Photoionization. Photoionization of the $1s$ shell of an ion (atom) with the spectroscopic symbol Z gives rise to the formation of an excited state $1s^2s^2p^m$. This state is regarded as an intermediate state which leads to the formation of ions $Z + 1$ (the state $1s^2s^2p^{m-1}$) as a result of spontaneous emission and ions $Z + 2$ (the states $1s^2s^2p^{m-2}$, $1s^2s2p^{m-1}$, and $1s^22p^m$) as a result of the Auger process. It is also assumed that the excited states $1s^2s^2p^{m-1}$ and $1s^22p^m$ decay instantaneously radiatively to the ground state $1s^2s^2p^{m-2}$. The autoionization probability w_z and spontaneous-emission A_z probability were calculated with the help of Cowan's program.⁷ The branching ratio, determin-

ing the relative rate of formation of the ions $Z + 2$ as a result of ionization of the $1s$ shell of the ions Z , is equal to

$$\delta_z = \frac{w_z}{A_z + w_z}. \quad (1.1)$$

The corresponding relative rate of formation of ions $Z + 1$ is equal to

$$1 - \delta_z = \frac{A_z}{A_z + w_z}. \quad (1.2)$$

Here

$$w_z = w_z^1 + w_z^2 + w_z^3,$$

where w_z^1 , w_z^2 , and w_z^3 are the probabilities of autoionization with formation of the states $1s^2s^2p^{m-2}$, $1s^2s2p^{m-1}$, and $1s^22p^m$.

We note that the exact values of A_z and w_z are not important for the ionization kinetics. It is important that $A_z \ll w_z$. In this case photoionization of the $1s$ shell of the ion Z results in formation of an ion $Z + 2$. Ions $Z + 1$ are formed primarily by electron-impact ionization of the outer shell of the ion Z ; decay A_z does not play a large role in their formation.

The rate of photoionization from the nl shell of the ion Z by radiation is equal to

$$R_{nl}^k = \int_{w_{nl}^k}^{\infty} \frac{J_u \sigma_{nl}^k(w)}{w} dw. \quad (1.3)$$

Here J_w is the spectral intensity of the incident radiation. The frequency of the incident radiation is connected with the energy $mv^2/2$ of the photoelectron by the relation $w = mv^2/2 + w_{nl}^k$, where w_{nl}^k is the threshold energy of ionization of an electron from the state characterized by the quantum numbers n, l of a particle of type k . The photoionization cross section as a function of the photon energy was calculated with the help of the ATOM program.⁸ The following approximations were employed for the photoionization of the N_2 molecule and the molecular ions N_2^+ and N_2^{++} :

$$\begin{aligned} R(N_2) &\approx 2R(N), \quad R(N_2^+) \approx R(N) + R(N^+), \\ R(N_2^{++}) &\approx R(N) + R(N^{++}). \end{aligned} \quad (1.4)$$

The following channels were assumed to be equally probable for the fractions of fragmentation of molecular ions by photoionization:

$$\begin{aligned} N_2^+ + h\omega &\rightarrow \begin{cases} N^{++} + N^{++} + 2e, \\ N^{+++} + N + 2e, \end{cases} \\ N_2^{++} + h\omega &\rightarrow \begin{cases} N^{+++} + N^{+++} + 2e, \\ N^{+++} + N^+ + 2e, \\ N^{++++} + N + 2e. \end{cases} \end{aligned}$$

The probability that an N^+ ion is formed in the process of fragmentation of an N_2 molecule is equal to 0.481:⁹

$$N_2 + h\omega \rightarrow \begin{cases} N^+ + N^+ + 2e, \\ N^{++} + N + 2e. \end{cases}$$

Ionization by electron impact. The cross sections adopted in this work for ionization by electron impact for N_2 , N , N^+ , N^{++} , N^{+++} , H_2 , and H are given in Refs. 10, 11, and 12. Lotz's formula¹¹ was employed for the cross section of the ionization process

$$N^{+++} + e \rightarrow N^{++++} + 2e.$$

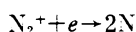
There are no data on the rates of impact ionization of molecular ions, so that in this work the following approximations were employed:

$$\begin{aligned} N_2^+ + e &\rightarrow N_2^{++} + 2e, \quad \sigma_{ion}(N_2^+) \approx \sigma_{ion}(N) + \sigma_{ion}(N^+), \\ N_2^{++} + e &\rightarrow N_2^{+++} + 2e, \quad \sigma_{ion}(N_2^{++}) \approx \sigma_{ion}(N) + \sigma_{ion}(N^{++}), \\ H_2^+ + e &\rightarrow 2H^+ + 2e, \quad \sigma_{ion}(H_2^+) \approx \sigma_{ion}(H), \\ H_3^+ + e &\rightarrow H_2^+ + H^+ + 2e, \quad \sigma_{ion}(H_3^+) \approx \sigma_{ion}(H_2). \end{aligned}$$

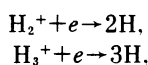
Dissociation. The cross section for the dissociation of N_2 molecules by electron impact was taken from Ref. 13, and the cross section for the same process in the case of H_2 molecules was taken from Ref. 14. The following approximation was employed for the rates of dissociation of H_2^+ and H_3^+ ions by electron impact:

$$\sigma_{dis}(H_2^+) \approx \sigma_{dis}(H_3^+) \approx \sigma_{dis}(H_2).$$

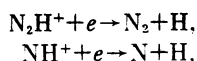
Dissociative recombination. The following processes were taken into account:



with the cross section from Ref. 15;

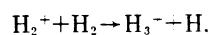


with the cross sections from Ref. 16, and

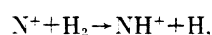


with the cross sections from Ref. 17.

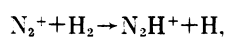
Conversion. The following processes were studied:



with the rate constant $\approx 2 \cdot 10^{-9} \text{ cm}^3/\text{s}$;¹⁸



with the rate constant $\approx 7 \cdot 10^{-10} \text{ cm}^3/\text{s}$;¹⁷ and,



with the rate constant $\approx 1.41 \cdot 10^{-9} \text{ cm}^3/\text{s}$.¹⁷

Charge exchange. Charge exchange of atomic and molecular ions with hydrogen atoms and molecules can appreciably reduce the rate of ionization. To take this process into account correctly it is necessary to know the charge-exchange cross sections at low temperature ($\approx 1 \text{ eV}$). However, the overwhelming majority of experimental information refers to energies $> 100 \text{ eV}$. The reactions considered are presented below together with the rate constants, which are taken from Ref. 17 and were estimated for an hydrogen-atom energy 1 eV :

$$\begin{aligned} N^+ + H &\rightarrow N + H^+, \quad k = 5 \cdot 10^{-10} \text{ cm}^3/\text{s}, \\ N^{++} + H &\rightarrow N^+ + H^+, \quad k = 5 \cdot 10^{-10} \text{ cm}^3/\text{s}, \\ N^{+++} + H &\rightarrow N^{++} + H^+, \quad k = 3.5 \cdot 10^{-9} \text{ cm}^3/\text{s}, \\ N^{++++} + H &\rightarrow N^{+++} + H^+, \quad k = 4 \cdot 10^{-9} \text{ cm}^3/\text{s}. \end{aligned}$$

2. BOLTZMANN'S EQUATION

Together with the system of kinetic equations for the ions we solved the nonstationary Boltzmann equation for a spherically symmetric electron-velocity distribution function $f(v, t)$ taking into account electron-electron collisions St_{ee} , electron-impact ionization of the particles St_{ion} , inelastic collisions St_{in} [the important channels are energy losses due to excitation of vibrational levels of H_2 , dissociation of H_2 and N_2 , etc. (Ref. 17)], elastic collisions St_{el} , recombination St_{rec} , and electron production due to photoionization and Auger processes St_f . Boltzmann's equation is written in the form^{19,20}

$$\frac{\partial f}{\partial t} = St_{ee} + St_{ion} + St_{in} + St_{el} + St_{res} + St_f. \quad (2.1)$$

In Eq. (2.1) the distribution function is normalized to the electron density

$$N_e = 4\pi \int_0^\infty f(v, t) v^2 dv, \quad (2.2)$$

and the fourth-order moment is the energy of the system:

$$E_e = 2\pi m \int_0^\infty f(v, t) v^4 dv. \quad (2.3)$$

The Coulomb collision integral has the form

$$St_{ee} = \frac{Y}{v^2} \frac{\partial}{\partial v} \left[I_0 f + \frac{v}{3} (I_2 + J_{-1}) \frac{\partial f}{\partial v} \right], \quad (2.4)$$

where

$$I_l = \frac{4\pi}{v^l} \int_0^v f y^{l+2} dy, \quad (2.5)$$

$$J_l = \frac{4\pi}{v^l} \int_v^\infty f y^{l+2} dy, \quad (2.6)$$

$$Y = \frac{4\pi e^4}{m^2} \ln \Lambda. \quad (2.7)$$

Here e and m are the electron charge and mass, respectively, and $\ln(\Lambda)$ is the Coulomb logarithm.

The ionization collision term was taken in the form

$$St_{ion} = \frac{1}{v^2} \sum_k N_k \left\{ \int_{(v^2+v_k^2)^{1/2}}^{(2v^2+v_k^2)^{1/2}} (v')^3 f(v') Q_k((v'^2-v^2-v_k^2)^{1/2}, v') \right. \\ \times \frac{v dv'}{(v'^2-v^2-v_k^2)^{1/2}} \\ \left. + \int_{(2v^2+v_k^2)^{1/2}}^{\infty} (v')^3 f(v') Q_k(v, v') dv' - v^3 \sigma_{ion}^k(v) f(v) \right\}. \quad (2.8)$$

Here N_k is the density of particles of type k which are ionized by electron impact, with a cross section $\sigma_{ion}^k(v)$; v_k is the threshold electron velocity; $Q_k(v, v')$ is the ionization differential cross section characterizing a process in which the ionizing electron has a velocity v' and the secondary electron has a velocity v .²¹ The electron with the lower energy is the secondary electron, i.e., the spectrum of secondary electrons extends from zero to $(v'^2 - v_k^2)^{1/2}/2$.

The total ionization cross section $\sigma_{ion}^k(v)$ can be expressed with the help of $Q_k(v, v')$ by the relation

$$\sigma_{ion}^k(v) = \int_0^{((v^2-v_k^2)/2)^{1/2}} Q_k(v, v') dv. \quad (2.9)$$

In this work we employed Opal's formula.²² This formula makes it possible to approximate the differential cross section $Q_k(v, v')$ with the help of the total cross section $\sigma_{ion}^k(v')$ which is known from experiment and works satisfactorily for N_2 and H_2 at all electron energies of interest to us:

$$Q_k(v, v') = \frac{\sigma_{ion}^k(v')}{\bar{v}^2 \arctg[(v'^2-v_k^2)/2\bar{v}^2]} \frac{2v}{[1+(v^2/\bar{v}^2)^2]}, \quad (2.10)$$

where \bar{v}^2 is a fit parameter which depends on the type of gas.

For inelastic collisions with particles of type k , having a threshold $\Delta E_{k,m}$ and a cross section $\sigma_{in}^{k,m}(v)$, the inelastic collision integral has the form

$$St_{in} = - \sum_{k,m} N_k \left\{ v \sigma_{in}^{k,m}(v) f(v) - \frac{v'^2}{v} \sigma_{in}^{k,m}(v') f(v') \right\}, \\ v' = (v^2 + 2\Delta E_{k,m}/m)^{1/2}. \quad (2.11)$$

Electron losses in recombination processes are described by the following collision integral:

$$St_r = - \sum_k N_k v f(v) \sigma_r^k(v). \quad (2.12)$$

Here N_k is the density of the corresponding molecular ions and $\sigma_r^k(v)$ is the cross section for the corresponding recombination process.

The elastic collision integral St_{el} was taken in the form²³

$$St_{el} = \frac{1}{4\pi v^2} \frac{\partial}{\partial v} \left[m^2 \sum_k \frac{N_k \sigma_{el}^k(v)}{M_k} v^4 f(v) \right. \\ \left. + m T_g \sum_k \frac{N_k \sigma_{el}^k(v)}{M_k} v^3 \frac{\partial f(v)}{\partial v} \right]. \quad (2.13)$$

Here N_k and M_k are, respectively, the density and mass of a molecule of type k ; $\sigma_{el}^k(v)$ is the cross section for elastic scat-

tering of an electron by a particle of type k ; and T_g is the temperature of the gas.

The source of electrons due to photoionization by x-rays has the form

$$St_f^1 = \frac{1}{4\pi v^2} \sum_k \frac{\sigma_f^k(v) N_k}{w} J_w. \quad (2.14)$$

The source of Auger electrons which arise in the process of photoionization of the inner shells by the incident radiation has the form

$$St_f^2 = \frac{1}{4\pi v^2} \sum_k N_k R_{nl}^k \frac{w_k}{w_k + A_k} \delta(v - v_{z,z+2}^k). \quad (2.15)$$

Here

$$\frac{m(v_{z,z+2}^k)^2}{2} = I_z^{1s} - I_z^{(nl)max} - I_{z+1}^{(nl)max}, \quad (2.16)$$

w_k is the probability of autoionization; A_k is the probability of spontaneous emission accompanying the transition of an electron from the L shell into the K shell; I_z^{nl} is the threshold energy, whose values were taken from Refs. 24 and 25; and, $\delta(v - v_{z,z+2}^k)$ is a delta function which determines the energy of the Auger electrons. Thus we obtain for the electron source

$$St_j = St_f^1 + St_f^2. \quad (2.17)$$

In the ion kinetic equations the rates of the corresponding processes were expressed in terms of the distribution function as follows:

$$v_k = 4\pi \int_0^{\infty} f(v) v^3 \sigma_k(v) dv. \quad (2.18)$$

3. HEATING OF THE GAS

It is easy to derive an equation for the temperature of the gas if it is assumed that all of the energy lost by electrons in elastic collisions goes into heating the gas. Then, in our notation,

$$\frac{dT_g}{dt} = \frac{1}{\sum_j c_j N_j} \left[\sum_k \int_0^{\infty} \frac{m^2 N_k \sigma_{el}^k(v)}{M_k} v^5 f(v) dv \right. \\ \left. + m T_g \sum_k \int_0^{\infty} \frac{N_k \sigma_{el}^k(v)}{M_k} v^4 \frac{\partial f(v)}{\partial v} dv \right] - \frac{T_g \sum_j c_j dN_j/dt}{\sum_j c_j N_j}. \quad (3.1)$$

Here T_g is the temperature of the gas in eV and N_j and c_j are, respectively, the density and heat capacity of heavy particles of type j .

We also assume that under the conditions of dissociative recombination the heavy particles appear in the ground state and all energy released in the reaction is transferred to the heavy particles as kinetic energy. Then an additional term of the form

$$\frac{1}{\sum_j c_j N_j} \sum_i \Delta E_i^{rec} v_i^{rec} N_i \quad (3.2)$$

appears in the temperature equation (3.1). Here $\Delta E_i^{\text{rec}} = I_i^{\text{ion}} - E_i^{\text{int}}$, where I_i^{ion} and E_i^{int} are the ionization potential and binding energy of a molecular ion of type i , and ν_i^{rec} and N_i are, respectively, the rate of recombination and the density of a molecular ion of type i . For the dissociative recombination reactions which are taken into account the ionization potential I_i^{ion} and the binding energy E_i^{int} were taken from Ref. 26.

We note that as the energy flux density of the radiation increases the gas temperature increases and can reach a level when thermal dissociation of hydrogen



becomes appreciable. For this reason we took this possibility into account with the help of rate constants for the direct and inverse reactions ($\text{M} = \text{H}_2$) from Ref. 27.

4. FLUORESCENCE MODEL

In the proposed method the fluorescence of the gas mixture in the region 300–550 nm was recorded. Emission of the second positive system of nitrogen N_2 and the first negative system of the N_2^+ ion falls within this spectral interval. The following processes were included in the kinetic equation for electronically excited molecular nitrogen $\text{N}_2(C^3\Pi_u)$:

- 1) electron-impact excitation of nitrogen from the ground state with the cross section from Ref. 28;
- 2) electron-impact ionization with the cross section from Ref. 29;
- 3) dissociation on neutral atoms, with the dissociation cross section for $\text{N}_2(C^3\Pi_u)$ assumed equal to the dissociation cross section of unexcited nitrogen with its own threshold ($E_{\text{diss}} = 1.1 \text{ eV}$);
- 4) photoionization with cross section equal to that of the unexcited molecule;
- 5) spontaneous transition of duration 41 ns to the lower state $B^3\Pi_g$ with emission of the second positive system.³⁰

The following processes were included in the kinetic equation for the electronically excited nitrogen ion $\text{N}_2^+(B^2\Sigma_u^+)$:

- 1) electron-impact excitation of the nitrogen ion in the process of ionization from the ground state of the N_2 molecule with the cross section from Ref. 31;
- 2) electron-impact ionization with the cross section equal to that of the unexcited ion;
- 3) photoionization with the cross section equal to that of the unexcited ion;
- 4) dissociative recombination with the cross section equal to that of the unexcited ion; and,
- 5) spontaneous transition of duration 63.1 ns to the ground state $X^2\Sigma_g^+$ with emission of the first negative system of N_2^+ (Ref. 30).

We note that many high-lying states of the hydrogen molecule which are excited by electron impact also emit photons in the indicated range of radiative decay. To determine this contribution to the fluorescence it must be compared with the contribution of electronically excited nitrogen to the fluorescence.

The maximum cross section for electron-impact excitation of the state $C^3\Pi_u$ of the N_2 molecule is equal to $0.4 \cdot 10^{-16} \text{ cm}^2$. The excitation energy for H_2 singlet states, which can be detected in the process of radiative decay, is

$E_{\text{exc}} \geq 13.7 \text{ eV}$ ($110\,480 \text{ cm}^{-1}$). This is the state $(2s)^2\Sigma_g^+$ ($E_{\text{exc}} = 99157.3 \text{ cm}^{-1}$) with maximum cross section for excitation by electron impact $\sigma_{\text{exc}}^{\text{max}} = 1.66 \cdot 10^{-19} \text{ cm}^2$.³² Since the cross section for the excitation of higher levels decreases, it is natural to expect that it will be even smaller for the levels of interest to us. In particular, the cross sections for a number of transitions of interest to us are presented in Ref. 33, and the maximum cross section does not exceed $4 \cdot 10^{-20} \text{ cm}^2$.

The maximum cross section for the excitation of the lowest triplet state of interest $d^3\Pi_u(3p)$ is equal to $4.2 \cdot 10^{-18} \text{ cm}^2$ at $E = 15.6 \text{ eV}$.^{32,34} Since the threshold for the excitation of the $d^3\Pi_u$ state of hydrogen is more than 2.5 eV higher than for the $C^3\Pi_u$ state of nitrogen, there is hope that the emission of this state of H_2 will not be more significant than radiative decay of the $C^3\Pi_u$ level. We have no data on the excitation cross sections for states lying above $d^3\Pi_u$. We can only conjecture that in the case of triplets the excitation cross section for the corresponding configurations will not exceed the cross sections for singlets.

5. NUMERICAL MODEL

The nonlinear system of kinetic equations for the ions can be formally written in the form

$$\frac{d\mathbf{N}}{dt} = \mathbf{F}(\mathbf{N}), \quad (5.1)$$

where \mathbf{N} is the vector of concentrations of the components of the gas mixture.

In a strongly nonequilibrium plasma the electron velocity distribution differs strongly from Maxwellian. This in turn affects the determination of the rates of reactions, included in Eq. (5.1), in which electrons participate. Therefore the system (5.1) must be solved simultaneously with the nonstationary Boltzmann equation for the spherically symmetric electron velocity distribution function (2.1) and the equation for the gas temperature (3.1).

The complete system of equations cannot be solved simultaneously without a computer. We note, however, that the system of equations (5.1) and (2.1) separates into two subsystems, which are different from the standpoint of numerical implementation. This is a system of ordinary differential equations (ODE) (3.1) and (5.1) and a partial differential equation for the electron velocity distribution function (2.1). In this work we made an attempt to obtain a unified numerical solution of the entire problem (2.1), (3.1), and (5.1). For this, the partial differential equation (2.1) was reduced by discretization in velocity space (while the time variable remains continuous) to a system of ordinary differential equations. The discretization is performed by the method of finite differences. It is well known that the system of ordinary differential equations obtained in this manner is a so-called "stiff" problem.³⁵ However, in the system of ordinary differential equations for the ion kinetics the rate constants of the processes often differ substantially (by several orders of magnitude), and this makes this system "stiff" also. For this reason the entire system obtained is "stiff" and powerful computational algorithms, like Geer's method,³⁶ can be used to solve it.

Geer's method is a linear multistep method. It is easy to show that such methods are conservative with respect to the particle number N_e and the energy of the system E , if the

right-hand side of Eq. (2.1) obtained after discretization conserves these quantities. Therefore it is desirable to preserve in the spatial difference approximation a number of the properties of Eq. (2.1). For example, if only the electron-electron collision integral St_{ee} is retained on the right-hand side of Eq. (2.1), then it can be shown that in such a system both the particle number N_e and the energy of the system E are conserved. If, however, only the inelastic collision integral St_{in} or only the elastic collision integral St_{el} is retained on the right-hand side of Eq. (2.1), then such a system conserves the particle number N_e . The following property is associated with the ionization term St_{ion} in Eq. (2.1):

$$4\pi \int_0^{\infty} v^3 St_{ion}(v) dv = \sum_k \nu_{ion}^k N_k. \quad (5.2)$$

Here ν_{ion}^k is the rate of ionization of the corresponding component of the gas mixture, determined by the formula (2.18), and N_k is the concentration of this component. It should be noted that the ionization rate ν_{ion}^k appears as a coefficient in the system of kinetic equations for the ions. For this reason, special attention must be devoted to matching the difference approximation of the ionization term St_{ion} and the difference approximation of the ionization rate ν_{ion}^k . If such matching is not achieved, it is possible to have a situation when the electron density N_1^e found from Eqs. (5.1) for the ion kinetics will differ strongly from the electron density N_2^e determined from Eq. (2.2). Since it is often impossible to determine beforehand which process can be neglected when solving a specific physical problem, it is important to take into account the conservation laws in the difference approximation of the corresponding terms. The question of constructing some conservative schemes for Eq. (2.1) was discussed in greater detail in Refs. 37 and 38. A modified LSODE program for solving ordinary differential equations was used for the numerical implementation of the proposed algorithm.³⁹ This program makes it possible to perform the integration with both variable step and variable order.

6. EXPERIMENTAL SETUP AND RESULTS

Experiments on recording the optical fluorescence of gases were performed on the Angara-5-1 setup. The soft-x-ray source was a dense hot plasma produced by implosion of an eight-wire aluminum liner with a linear mass $150 \mu\text{g}/\text{cm}$ and a diameter 20 mm. The total radiation energy was recorded with integral calorimeters and was equal to $\sim 100 \text{ kJ}$. The time dependence and spectral characteristic of the soft x rays were measured with the help of x-ray vacuum diodes (XVD) behind different filters. The width of the soft-x-ray pulse was $\sim 40 \text{ ns}$, and the temporal resolution of the measuring channel was not worse than 5 ns.

The radiation source was the 1–3 cm high pinch with diameter $\leq 4 \text{ mm}$ (depending on the conditions of the experiment) formed on the axis of the system. Measurements performed before the appearance of the intense soft x rays showed that the electrons in the system emit hard bremsstrahlung, which arises as a result of electron leakage in the course of establishing magnetic confinement in the output system. Experiments on the implosion of multiwire liners and the characteristics of their soft-x-ray emission are described in greater detail in Refs. 4 and 5.

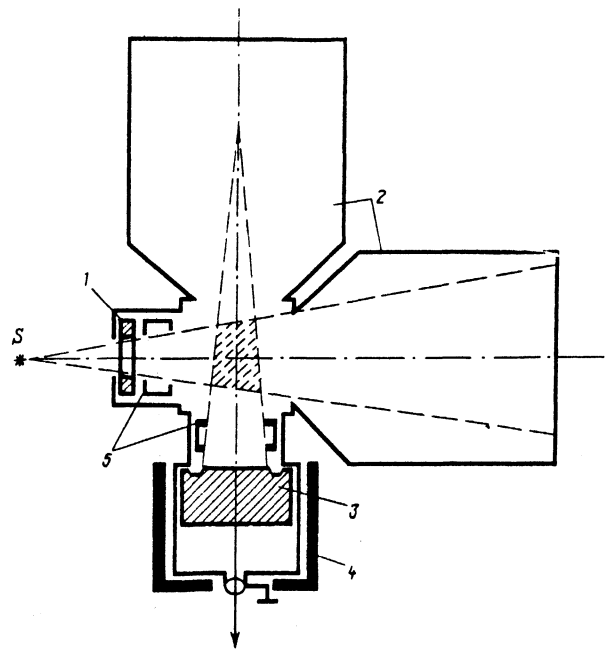


FIG. 1. Layout of the experimental setup. S is the source, 1 is the input window with a filter, 2 are optical traps, 3 is a SDF-7 photocell, 4 is a lead screen, and 5 is a system of diaphragms.

The gas studied was located in the chamber shown in Fig. 1. The chamber had an attachment for evacuation and injection of the gas mixture and for checking the mixture pressure. Spectrally pure gases were employed in the experiment. The fluorescence was recorded with an SDF-7 photocell, which recorded radiation with wavelengths of 300–600 nm. The observation axis of the photocell made an angle 90° with the axis of the input window. To reduce the effect of hard x-rays the photocell was surrounded with 6 mm thick lead plates. A collection of diaphragms was used to isolate for study a region of the gas mixture with a volume of 1–2 cm^3 . The parasitic signal arising as a result of the scattering of light and explosion of the surface of the chamber under

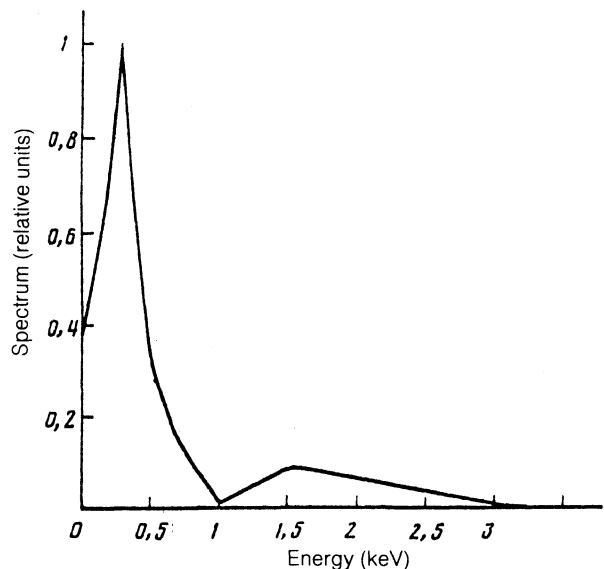


FIG. 2. Spectral intensity of the radiation from the liner (in arbitrary units).

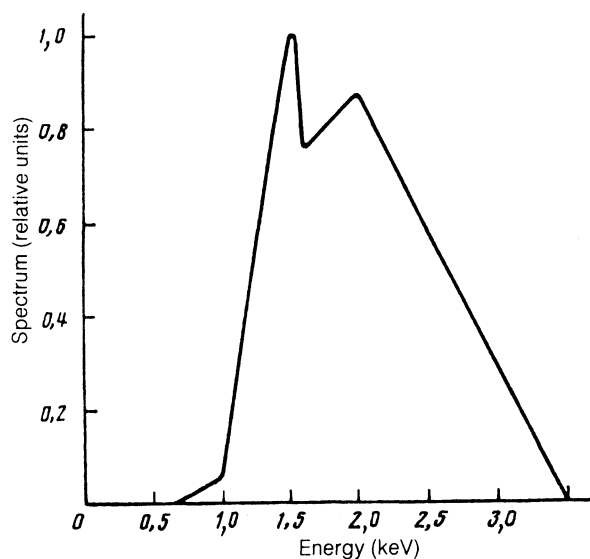


FIG. 3. Spectral intensity of radiation after the filters (in arbitrary units).

the action of powerful radiation fluxes was reduced with the help of a combination of the system of diaphragms and traps for soft x rays and light.

The input window of the chamber was covered with vacuum-tight filters made of 2- μm thick Al-coated lavsan polyester. During the experiments the radiation destroyed the filters, so that they had to be replaced before each shot. The input window of the chamber was located several centimeters from the source; this made it possible to obtain soft-x-ray fluxes with photon energy $h\nu \geq 1$ keV and an intensity of 1–2 J/cm².

The spectral intensity of the radiation from the liner is presented in Fig. 2, and the spectral intensity of the radiation past the filters and acting directly on the gas is presented in Fig. 3. In control shots conducted with no gas mixture in the chamber a signal of amplitude 0.4–2 V was recorded from the photocell during the main voltage pulse on the concentrator of the Angara-5-1 setup.

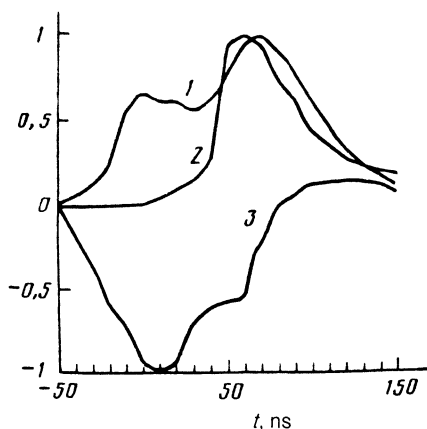


FIG. 4. Oscillograms of fluorescence of the gas mixture 4.4% N₂ + 95.6% H₂ with a pressure of 21 Torr (the maximum signal is ~1 V) (1), the signal from the x-ray vacuum diode recording soft x-rays from the liner (2), and the voltage on the concentrator of the Angara-5-1 setup (the maximum signal is ~10⁶ V) (3). All curves are given in arbitrary units.

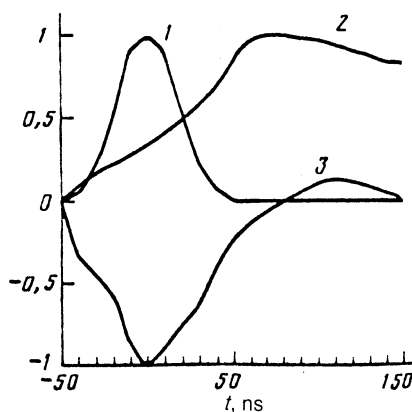


FIG. 5. Same as Fig. 4 but with a gas pressure $\sim 10^{-3}$ Torr.

Two groups of control experiments were performed to determine the nature of the signal. In the first group the light channel was covered. In the second group the light channel was open and the radiation from residual gas with a pressure of 10^{-4} – 10^{-3} Torr could be observed. As a result, it was established that the signal is not related with fluorescence in the volume of the chamber and is caused by the hard x-rays which are produced. This proposition is also supported by the fact that it was observed only when a voltage was present on the output unit of the setup. This signal is superposed on the useful fluorescence signal from the gas. Figure 4 shows oscillograms of the fluorescence of the mixture 4.4% N₂ + 95.6% H₂ with a pressure of 21 Torr, the signal from the x-ray vacuum diode (which records the soft x-rays from the liner), and the voltage on the concentrator of the Angara-5-1 setup.

The signal from the SDF-7 photocell has two peaks. The control experiments showed that the first peak is associated with the x-rays and its width does not exceed that of the voltage pulse. As one can see from Fig. 5, the voltage becomes negligibly small by the time of the second peak. This means that the contribution of hard x-rays to the signal does not exceed several percent at the moment of the second

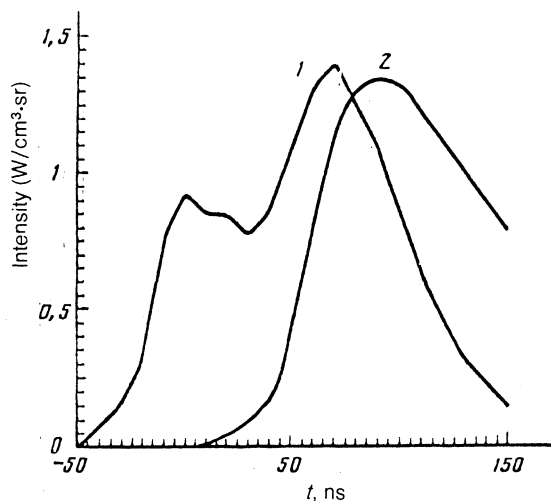


FIG. 6. Fluorescence of the gas mixture 4.4% N₂ + 95.6% H₂ with a pressure of 21 Torr. 1—Experiment, 2—numerical calculation.

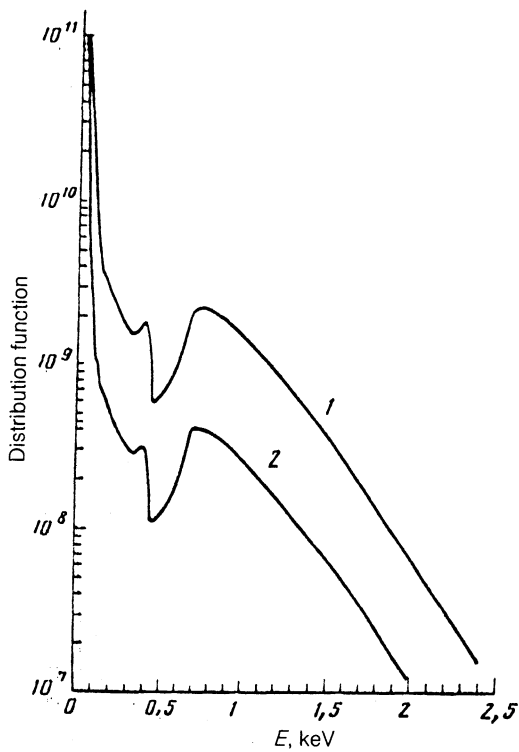


FIG. 7. Electron energy distribution function at different times: $t = 51.02$ ns (1) and $t = 147.01$ ns (2).

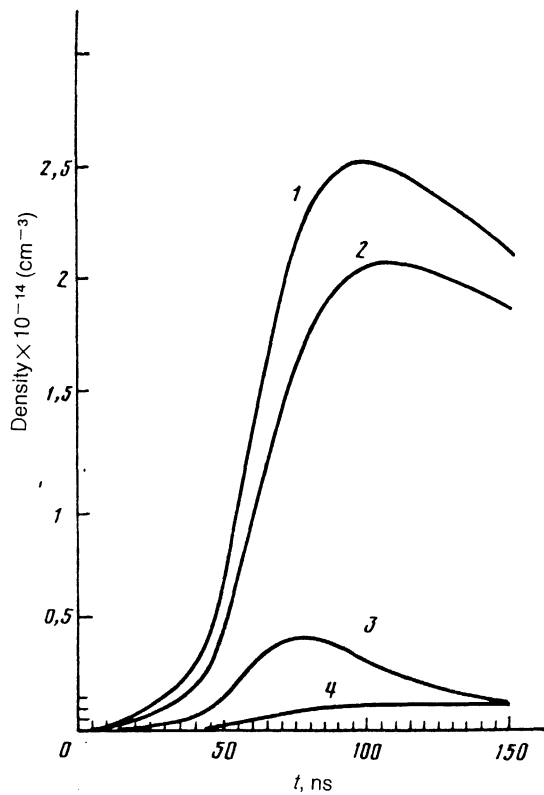


FIG. 8. Density of the principal ions of the starting gas mixture at different times: Electron density N_e (1), H_3^+ ion density (2), N_2H^+ ion density (3), and NH^+ ion density (4).

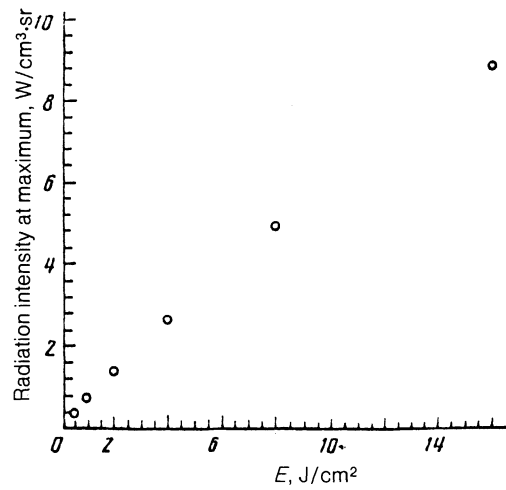


FIG. 9. Computed maximum fluorescence of the starting gas mixture as a function of the intensity soft-x-ray intensity.

minimum and later. Unfortunately, the available information does not make it possible to determine the behavior of the fluorescence signal from the leading edge of the pulse. This can be done, in principle, with the help of a second identical measurement channel, in which the light signal is covered, or by increasing the thickness of the lead screen surrounding the SDF-7 photocell.

The mathematical model described above agrees well with experiment. Figure 6 shows as a function of time the fluorescence recorded in the experiment (Fig. 1) and the computed fluorescence intensity (Fig. 2). In the plot the time is given in nanoseconds and the intensity in units of $W/(cm^3 \cdot sr)$. We note that the absolute values of the radiation maxima in the experimental and theoretical curves are virtually identical. The small discrepancy in the position of the fluorescence maximum can be explained by the fact that in the calculations the energy spectrum of the incident radiation, taken in accordance with Fig. 3, is constant in time, whereas in the experiment it could be time dependent.

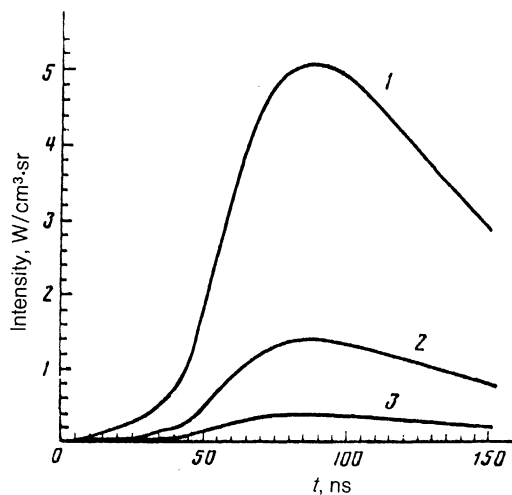


FIG. 10. Time dependence of the fluorescence intensity for different mixtures $H_2 + N_2$: 1) $H_2:N_2 = 10:1$, $P = 22$ Torr; 2) $H_2:N_2 = 20:1$, $P = 21$ Torr; and, 3) $H_2:N_2 = 40:1$, $P = 20.5$ Torr.

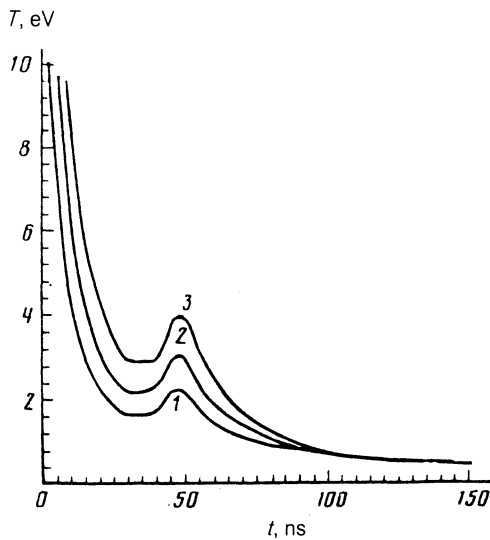


FIG. 11. Time dependence of the electron temperature for the same mixtures as in Fig. 10.

Figure 7 shows the electron energy distribution function at different times. It differs significantly from the equilibrium distribution function. The high-energy tail of the distribution function is determined mainly by the spectrum of the incident x rays. The small maximum near ≈ 0.4 keV is associated with the presence of Auger electrons. The forms of the curves are similar because the energy spectrum of the incident radiation does not change with time.

Figure 8 shows the computed time dependences of the ionic composition of the gas mixture and the electron density. In the plot time is given in nanoseconds and the electron density in cm^{-3} . One can see that under the conditions of the experiment the principal ions are H_2^+ , N_2H^+ , and NH^+ , while the contribution of other ions is insignificant.

The good agreement between the experimental and computed fluorescence curves shows that the proposed mathematical model adequately describes the real processes occurring in the gas mixture under the action of an x-ray pulse. For the present mixture of gases we performed a series of calculations showing that the fluorescence of the gas mixture in the converter is a linear function of the intensity of the incident radiation in the flux interval $0\text{--}16$ J/cm^2 (see Fig. 9). This gives hope that this experimental method of recording and measuring the intensity of the incident x-rays will find further applications.

Subsequent calculations showed that the intensity of the fluorescence of the gas mixture is sensitive to the nitrogen content in the mixture with the same concentration of buffer gas (hydrogen). Figure 10 shows the computed time dependences of the fluorescence intensity in different gas mixtures. Curve 1 corresponds to the fluorescence of a gas mixture with a pressure of 22 Torr ($\text{H}_2:\text{N}_2 = 10:1$). Curve 2 corresponds to fluorescence with a pressure of 21 Torr ($\text{H}_2:\text{N}_2 = 20:1$). Curve 3 corresponds to fluorescence with a pressure of 20.5 Torr ($\text{H}_2:\text{N}_2 = 40:1$). We note that the change in the intensity of fluorescence is not directly proportional to the change in the absolute nitrogen concentration in the gas mixture. Figure 11 shows the time dependence of the electron temperature for the mixtures described above. The

maximum in the electron temperature is related with the temporal shape of the incident x-ray pulse.

- ¹D. R. Westervelt and H. Hoerlin, Proc. IEEE **53**, 2287 (1965).
- ²S. L. Davydov [Ed.], *Nuclear Explosions in Space, on the Ground, and Underground* [in Russian], Voenizdat, Moscow, 1974.
- ³A. V. Zhemerov and B. M. Stepanov, *Physics of Pulsed Radiative Excitation of Fluorescence of Air* [in Russian], Energoatomizdat, Moscow, 1984.
- ⁴I. K. Aivazov, V. D. Vikharev, G. S. Volkov *et al.*, Fiz. Plazmy **16**, 645 (1990) [Sov. Phys. Plasma Physics **16**, 373 (1990)].
- ⁵I. K. Aivazov, V. D. Vikharev, G. S. Volkov *et al.*, Fiz. Plazmy **14**, 197 (1988) [Sov. Phys. Plasma Physics **14**, 110 (1988)].
- ⁶V. D. Vikharev, S. V. Zakharov *et al.*, Zh. Eksp. Teor. Fiz. **99**, 1133 (1991) [Sov. Phys. JETP **72**(14), 631 (1991)].
- ⁷R. D. Cowan, *The Theory of Atomic Structure and Spectra*, Univ. of California (1981).
- ⁸L. A. Vaĩnshtein and V. P. Shevel'ko, *Structure and Characteristics of Ions in Hot Plasma* [in Russian], Nauka, Moscow, 1986.
- ⁹W. Eberhardt, J. Stohr, J. Feldhaus *et al.*, Phys. Rev. Lett. **51**, 2370 (1983).
- ¹⁰E. Brook, M. F. A. Harrison, and A. C. H. Smith, ICPEAC X, Paris (1977), p. 1078.
- ¹¹W. Lotz, Astrophys. J. Suppl. **14**, Suppl. **128**, 207 (1967).
- ¹²S. P. Khare and J. A. Kumar, J. Phys. B **10**, 2239 (1977).
- ¹³L. S. Polak, A. A. Ovsyannikov, D. D. Slovetskii, and F. B. Vurzel', *Theoretical and Applied Plasma Chemistry* [in Russian], Nauka, Moscow, 1975.
- ¹⁴J. B. Corrigan, J. Chem. Phys. **43**, 4381 (1965).
- ¹⁵B. M. Smirnov, *Ions and Excited Atoms in Plasma* [in Russian], Atomizdat, Moscow, 1974.
- ¹⁶A. V. Elets'kiĩ and B. M. Smirnov, Usp. Fiz. Nauk **136**, 25 (1982) [Sov. Phys. Usp. **25**(1), 13 (1982)].
- ¹⁷H. Tawara, T. Kato, and Y. Nakai, Atomic Data and Nuclear Data Tables **32**, 235 (1985).
- ¹⁸A. V. Dem'yanov, N. A. Dyatko, I. V. Kochetov *et al.*, Fiz. Plazmy **11**, 361 (1985) [Sov. Phys. Plasma Physics **11**, 210 (1985)].
- ¹⁹I. Shkarovskii, T. Dzhonston, and M. Bachinskii, *Kinetics of Plasma Particles* [in Russian], Atomizdat, Moscow, 1969.
- ²⁰A. V. Gurevich and A. B. Shvartsburg, *Nonlinear Theory of Propagation of Radio Waves in the Ionosphere* [in Russian], Nauka, Moscow, 1973.
- ²¹N. A. Dyatko, I. V. Kochetov, A. P. Napartovich, and M. D. Taran, Preprint IAE-3842/12, Moscow, 1983.
- ²²C. B. Opal, W. K. Peterson, and E. C. Beaty, J. Chem. Phys. **55**, 4100 (1971).
- ²³Yu. P. Raĩzer, *Physics of Gas Discharges* [in Russian], Nauka, Moscow, 1987.
- ²⁴C. E. Moore, Atomic Energy Levels, Circular of NBS, 467, Washington (1948), Vol. 1; Vol. 2 (1952); Vol. 3 (1958); Rept. NSRDS-NBS 34 (1970).
- ²⁵W. Lotz, JOSA **58**, 915 (1968).
- ²⁶B. M. Smirnov, *Complex Ions* [in Russian], Nauka, Moscow, 1983.
- ²⁷V. N. Kondrat'ev, *Handbook of Rate Constants of Gas-Phase Reactions* [in Russian], Nauka, Moscow, 1971.
- ²⁸D. C. Cortwright, S. Trajmar, A. Chytjion, and W. Williams, Phys. Rev. A **16**, 1041 (1977).
- ²⁹L. A. Vaĩnshtein, N. I. Sobel'man, and E. A. Yukov, *Excitation of Spectral Atoms and Spectral Line Broadening* [in Russian], Nauka, Moscow, 1979, p. 181.
- ³⁰L. A. Kuznetsova, N. E. Kuz'menko, Yu. Ya. Kuzyakov, and Yu. A. Plastinin in *Probabilities of Optical Transitions in Diatomic Molecules* [in Russian], edited by R. V. Khokhlov, Nauka, Moscow, 1980, p. 162.
- ³¹A. V. Zhemerov and B. M. Stepanov, *Physics of Pulsed Radiative Excitation of Fluorescence of Air* [in Russian], Energoatomizdat, Moscow, 1984, p. 14.
- ³²S. Chung *et al.*, Phys. Rev. A **12**, 1340 (1975).
- ³³R. L. Day, R. J. Andersen, and F. A. Sharpston, J. Chem. Phys. **71**, 3683 (1979).
- ³⁴G. R. Mohlmann and F. Y. de Gler, Chem. Phys. Lett. **43**, 240 (1976).
- ³⁵K. Dekker and J. Verwer, *Stability of Runge-Kutta Methods for Stiff Nonlinear Differential Equations*, American Elsevier, N.Y., 1984.
- ³⁶E. Hairer, S. Nersett, and G. Wanner, *Solving Ordinary Differential Equations*, Springer-Verlag, N.Y., 1986.
- ³⁷A. V. Bobylev and V. A. Chuyanov, Zh. Vychisl. Matem. Matem. Fiz. **16**, 407 (1976).
- ³⁸A. V. Bobylev, I. F. Potapenko, and V. A. Chuyanov, Dokl. Acad. Nauk SSSR **255**, 1348 (1980) [Sov. Phys. Dokl. **25**(12), 994 (1980)].
- ³⁹A. C. Hindmarsh, ACM Signum Newsletter **15**, No. 4 (1980).

Translated by M. E. Alferieff